Fano resonances and electromagnetically-induced transparency in silicon waveguides loaded with plasmonic nanoresonators

Rubén Ortuño, Mario Cortijo, Alejandro Martínez

Nanophotonics Technology Center, Universitat Politècnica de València, Camino de Vera s/n, Valencia 46022, Spain

Email: amartinez@ntc.upv.es

Abstract:

The fundamental electric dipolar resonance of metallic nanostrips placed on top of a dielectric waveguide can be excited via evanescent wave coupling, thus giving rise to broad dips in the transmission spectrum of the waveguide. Here we show via numerical simulations that narrower and steeper Fano-like resonances can be obtained by asymmetrically coupling in the near field a larger nanostrip - supporting an electric quadrupole in the frequency regime of interest - to the original, shorter nanostrip. Under certain conditions, the spectral response corresponding to the electromagnetically-induced transparency phenomenon is observed. We suggest that this hybrid plasmonic-photonic approach could be especially relevant for sensing or all-optical switching applications in a photonic integrated platform such as silicon photonics.

1. Introduction

Metallic nanostructures support localized surface plasmon resonances (LSPRs) at visible and near-infrared wavelengths. Such LSPRs are mainly characterized by large scattering and absorption cross-sections as well as strong field localization in deep-subwavelength volumes [1][2]. This last feature gives rise to an extreme sensitivity of the LSPR to tiny variations in the surrounding dielectric medium, which makes such nanostructures highly appropriate for many photonic applications, remarkably including biosensing [3] and non-linear optics [4]. Due to its subwavelength size, exciting and measuring the response of an isolated single plasmonic nanostructure becomes difficult, which poses an enormous challenge in realizing independent excitation and measurement of multiple subwavelength-sized nanostructures in parallel [5][6]. This is why measurements of LSPRs spectra as well as their associated wavelength shifts employed in sensing are typically carried out on two dimensional arrays of decoupled metallic nanostructures that are simultaneously illuminated so that an average response can be recorded [7][8]. This approach enormously simplifies the measurements but the drawback is that the striking features of single nanostructures and their associated LSPRs are lost.

This limitation may be overcome by exciting the nanostructure via high-index dielectric waveguides with transverse dimensions of the order of half of the wavelength. This hybrid plasmonic-photonic approach would enable the excitation and measurement of multiple nanostructures in parallel and in real time, including the possibility of using different wavelengths, amplitudes and phases for independently driving each nanostructure [9]. Moreover, if implemented on a silicon photonics platform, it would enable to fabricate plasmonic devices by using standard semiconductor fabrication tools (such as Complementary Metal Oxide Semiconductor processes), with the added benefits of low-cost and mass-volume production [10][11].

Several experimental demonstrations of excitation of the LSPR of plasmonic nanostructures placed on top of high-index waveguides in the visible and near-infrared regimes have been recently reported [12]-[17]. In this configuration, the excitation of the metallic element takes place because of the near-field coupling between the nanostructure dipolar LSPR and the evanescent field of the waveguide, which supports the propagation of the fundamental transverse electric (TE) mode with a main electric field component parallel to the chip plane and transverse to the propagation direction. Such evanescent field coupling is generally weak so waveguide-nanostructure interaction efficiencies are quite low (<20% per nanostructure [15][16]), resulting in small extinction ratios in the transmission spectrum. Additionally, ohmic

losses in the metal results in broad resonances, which may hinder practical applications where narrow resonances are required. Larger extinction ratios (or deeper dips in the transmission spectrum) can be achieved, for instance, by placing several nanostructures on top of the waveguide [12],[14],[17] or by embedding the nanostructure inside of the waveguide [18],[19]. However, strategies for narrowing the LSPR linewidth as well as sharpening its spectral profile have not been yet addressed within this hybrid plasmonic-photonic approach.

It has been recently shown that narrower Fano-like resonances exhibiting an asymmetric profile [20]-[21] can be obtained by coupling bright and dark plasmonic resonances, playing typically the fundamental electric dipolar LSPR the role of the bright mode and higher-order LSPRs (magnetic dipole [22] or electric quadrupole [23],[24]) the role of the dark mode. Under this approach, a phenomenon analog to the electromagnetically-induced transparency (EIT) occurring in quantum optics has been observed: a high-transmission narrow peak is obtained within a broad spectral region with high absorption [25]. Sharp spectral characteristics displayed by Fano resonances or EIT peaks have been used to improve the performance of plasmonic devices such as biosensors [26] or optical switches [27].

In this work, we show via numerical simulations that asymmetric Fano-like resonances as well as EIT behavior are obtained in the transmission spectrum of silicon waveguides loaded by coupled plasmonic nanostrip pairs. The nanostrips lengths are chosen to support both a dipolar (short nanostrip) and a quadrupolar (long nanostrip) resonances at the wavelength of interest (telecom regime). We show that when the nanostrips are coupled in a symmetric configuration the quadrupolar mode is not excited. This situation changes when an asymmetry is introduced so that dipolar currents in the short nanostrip excite the otherwise dark quadrupolar mode, then producing asymmetric spectral features in transmission as well as, ultimately, an EIT peak.

2. Dipolar plasmon resonance by an isolated nanostrip

Figure 1a shows a schematic of the starting configuration: a short gold (Au) nanostrip of length l_1=85nm, with square cross-section $d_1=h$=30nm, placed on top of a silicon waveguide with rectangular cross-section (w=500nm and t=190nm). The full system is placed on a silica substrate, as is the typical case in devices built on silicon-on-insulator wafers. All numerical simulations in this work have been performed using the commercial 3-D full-wave solver CST Microwave Studio, which implements the finite integration technique. The dimensions of the nanostrip are chosen so that the structure exhibits a transmission dip at wavelengths around 1,500 nm. Such a dip occurs because at those wavelengths the evanescent field of the guided mode of the waveguide excites a plasmonic resonance of the metallic element, which results

in that part of the guided field is either scattered out of the waveguide or absorbed. The calculated transmission spectra - considering excitation of the fundamental TE mode of the waveguide for a single nanostrip - are shown in Fig. 1b. It can be seen that maximum interaction is achieved when the nanostructure is perfectly symmetric with respect to the yz-plane (Δx_1=0) since it is in this position where the evanescent field of the fundamental TE waveguide mode is stronger [28]. The interaction efficiency (or extinction ratio), η, defined as the optical power that is drawn from the waveguide due to the presence of the nanostructure mainly because of out-of-plane scattering and absorption, reaches a maximum value around 0.12, in agreement with previous works [15],[16]. As long as the nanostructure is shifted laterally, the dip becomes shallower and η decreases because of the weaker interaction between the guided mode and the nanostructure LSPR, to become finally negligible when the nanostructure approaches the waveguide boundary. Stronger interactions can be achieved by placing several nanostrips on the waveguide, as depicted in Fig. 1c, which also shows that decreasing the thickness t of the silicon waveguide also increases η above 0.6 because the field confinement inside the waveguide core is reduced and, as a result, the interaction between guided field and resonant element increases.
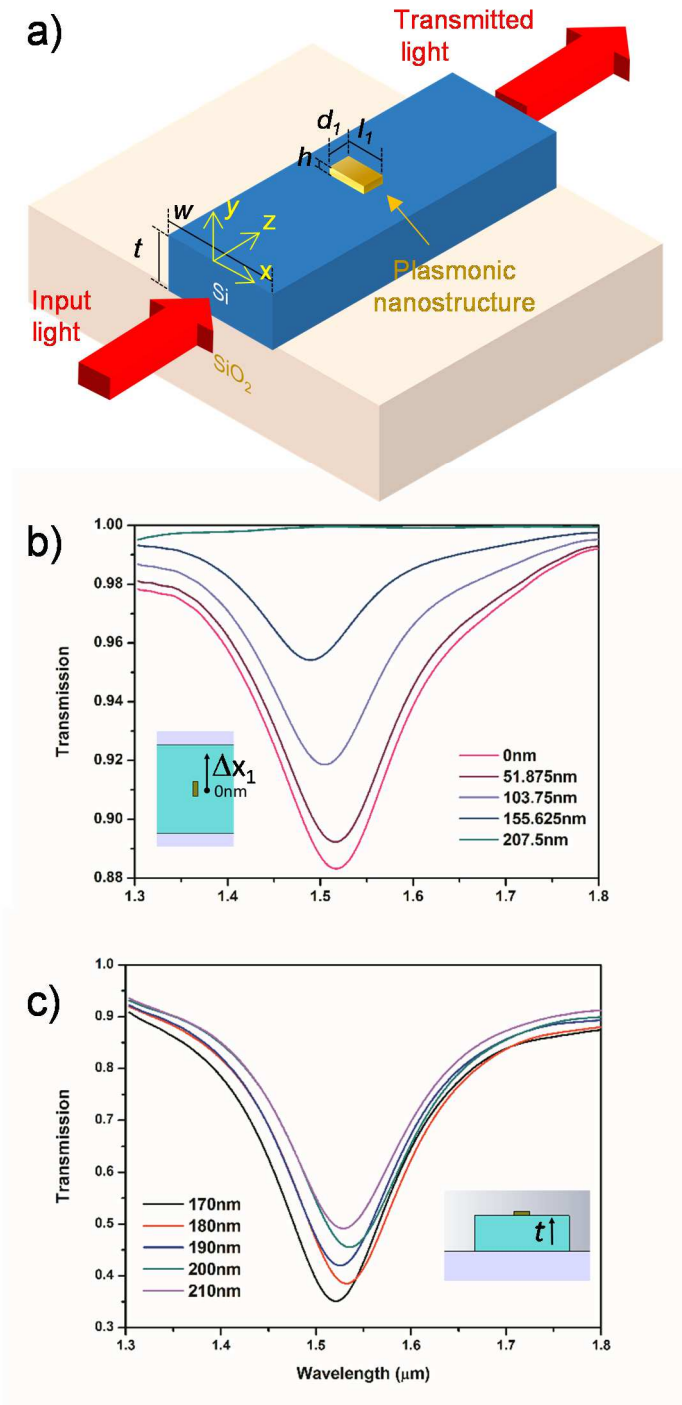
Figure 1. (a) Scheme of the structure under study: a single gold nanostrip on top of a silicon waveguide produces a dip in the transmission spectrum (b) because of the excitation of the electric dipolar resonance of the nanostrip. (c) The transmission dip gets deeper (larger extinction ratio) when placing five nanostrips separated by 155 nm. (b) and (c) depict several curves corresponding to lateral displacements of the nanostrip (Δx_1) and different thicknesses of the silicon waveguide (t), respectively. All the curves are normalized transmission obtained as the ratio between the transmission spectra with and without nanostructure.

3. Fano resonance and EIT behavior by coupling a second nanostrip

Now, a second Au nanostrip with a length of l_2=220nm is placed 20nm away from the previous nanostrip, as depicted in Fig. 2a. When both nanostrips are placed symmetrically with respect to the axis of the waveguide, the transmission through the waveguide slightly varies from the case of the single short nanostrip of 85nm, as shown in Fig. 2c. Only a small wavelength shift is observed as a result of the inclusion of a second scatterer. We have checked that this behavior is kept regardless of the length of the longer Au nanostrip and its distance to the short one as shown on Fig. 3b. However, a Fano response arises when the nanostrips are placed asymmetrically with respect to the axis of the waveguide. This is the case, for instance, of the configuration shown in Fig. 2b, in which $\Delta x_1 \neq 0$ for the short nanostrip, and which transmission spectrum is depicted in Fig. 2d. It should be remarked that the long nanostrip is never excited when isolated by the light travelling through the waveguide nor in the symmetric or asymmetric configuration, as can be seen in the red curves of Fig. 2c and Fig. 2d. This means that the dark mode of the large nanostrip is only excited by its near-field coupling to the short nanostrip bright mode, as long as its length l_2 supports an electric quadrupolar mode. It has to be mentioned that when nanotrips get coupled the position of the spectral features and the degree of asymmetry of the Fano-like transmission spectrum can be controlled by changing the gap separating the nanostrips, which modifies the coupling strength as depicted in Fig. 3a and 3c.
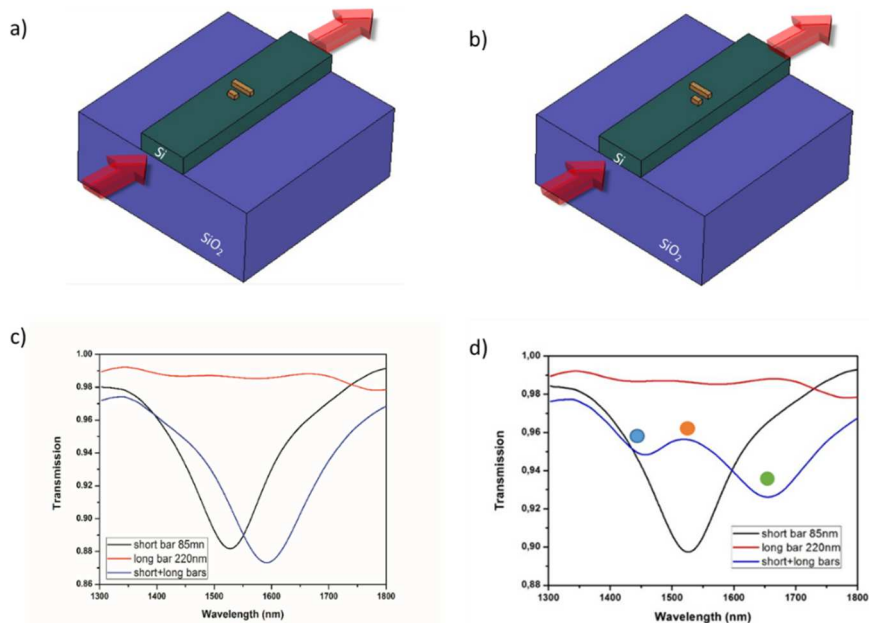

Figure 2. Schematic with the two coupled nanostrips on the silicon waveguide with (a) symmetric and (b) asymmetric - $\Delta x_1 \neq 0$ for the short nanostrip - configuration. The blue curve represents the transmission for the (c) symmetric configuration showing no Fano effects and for the (d) asymmetric configuration showing Fano effects. Also, in black (red) the case when only the short (long) nanostrip is considered on top of the silicon waveguide.
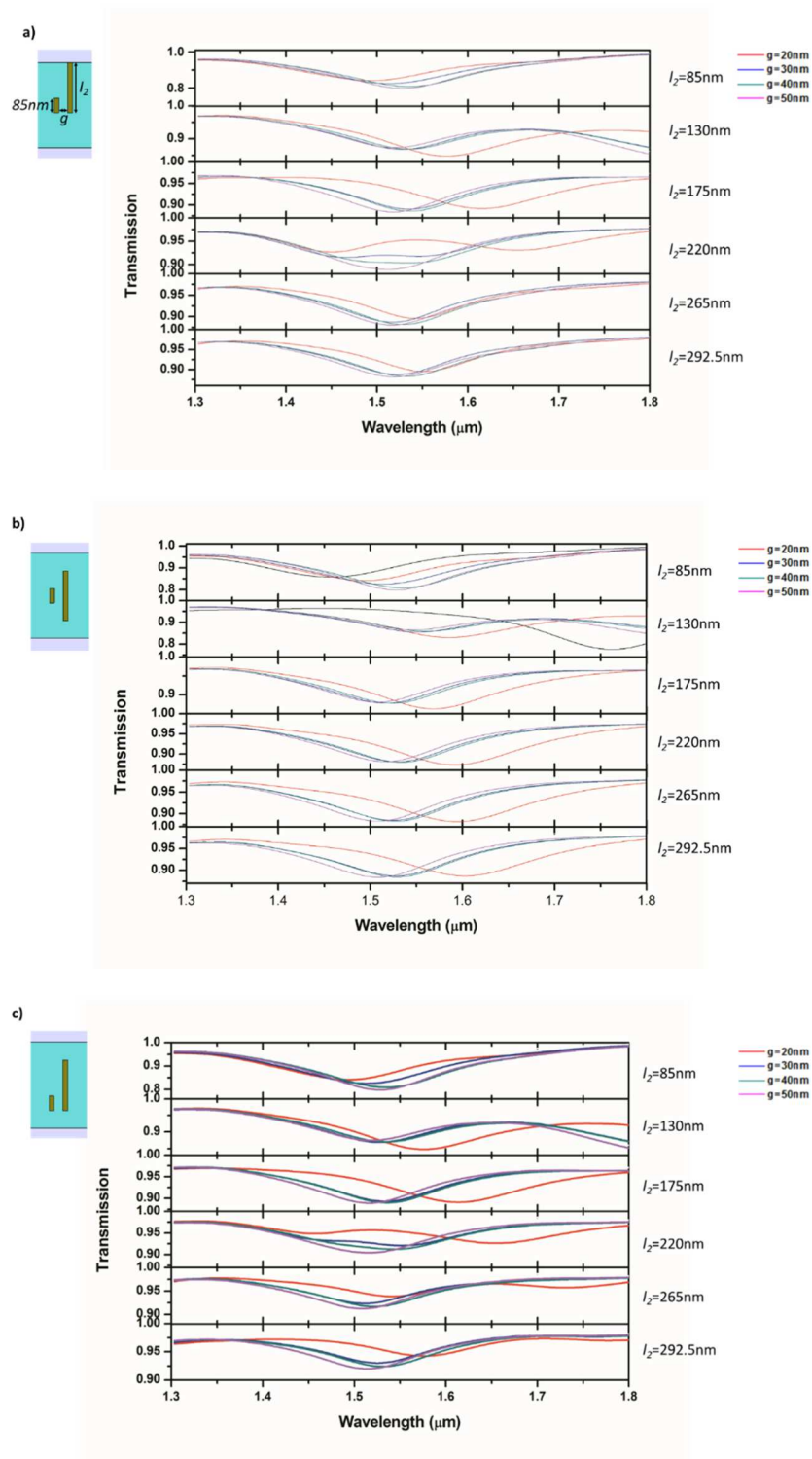
Figure 3. Variation of the transmission with the long nanostrip length l_2 and its separation g to the short nanostrip, with the short (a), both (b), or the long (c) nanostrips centered in the middle of the waveguide as depicted in the sketch of each figure. Notice that the right selection of the physical dimensions of the coupled system can give rise to the pursued Fano response.

To get a deeper insight on the origin of the Fano resonance arisen when coupling the nanostrips, we have investigated the current and electric field distributions along the metallic elements at

the wavelengths highlighted in Fig. 2d. The quadrupolar nature of the resonance exhibited by the long nanostrip is clearly seen in Fig. 4, also showing that such resonance is excited via near-field coupling with the bright dipolar resonance of the short nanostrip. Moreover, the destructive interference in the resonator system gives rise to a narrow EIT-like window around 1,540nm (orange circle in Fig. 2d) [29], in coincidence with the wavelength for which the isolated short nanostrip gives a maximum extinction ratio. The destructive interference can be proved by the comparison of the phase surface current distributions, which reveals that the roll-off of the transmittance at the EIT window is due to the phase change of the field distribution at those frequencies, and by the decay of the net current flowing in the parallel direction to the nanostrips at the EIT wavelength. This is proved by computing the current at, for instance, the middle of the short nanostrip, which varies from 1.159mA, 0.735mA and 1.54mA, respectively at the wavelengths marked with blue, orange and green colours in Fig. 2d. In systems in which the plasmonic ensemble showing a Fano resonance is placed in a homogeneous medium, an almost complete cancellation of the current through the metallic element showing the dipolar resonance is feasible at the EIT peak [24]. Here, however, we only observe a reduction of the total current. We think that this can be explained by assuming that the high-index substrate (the silicon waveguide) induces the formation of image currents that together with the real currents along the nanostrip would result in an almost complete cancellation of the dipolar moment at the EIT wavelength. Since our plasmonic nanostructures are placed on silicon-on-insulator substrates showing multiple dielectric interfaces, the situation would become more complex than in plasmonic structures deposited on continuous dielectric substrates [30]-[32], because of the appearance of multiple image currents (see schematic diagram on Fig. 5). A more detailed analysis including such image currents would provide more insights into the EIT behavior in this kind of system but this is definitely beyond the scope of this work.

To further support the Fano interpretation of the nanostrip coupled system, Fig. 6 depicts its extinction and absorption coefficients. Due to simulation constraints, such spectra were computed assuming that the nanostrips were completely surrounded by an effective index medium with n_{eff}=2.32 - which is the effective index of the TE-like guided mode feeding the waveguide at the LSPR wavelength of the short nanostrip - and illuminated by a plane wave [32]. This choice was made to spectrally place the LSPR at the same wavelengths as in the guided system. As shown in Fig. 5, the observed wavelength shift between maxima of the scattering and absorption spectra is also a clear signature of the Fano response of the coupled system [6].
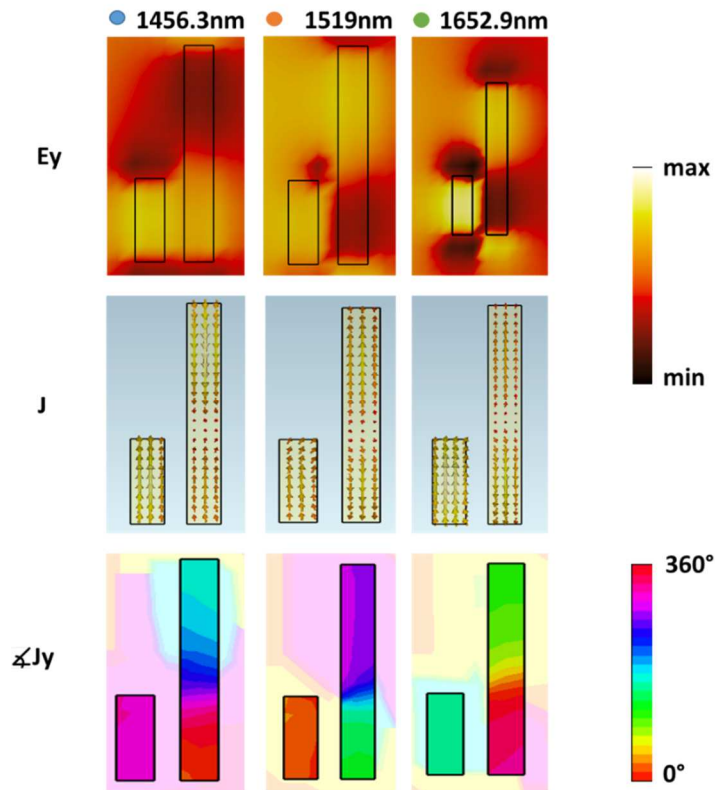
Figure 4. Electric field's parallel component to the nanostrips (top), surface current distribution (middle) and phase of the surface current distribution parallel component to the nanostrips (down) computed at three different wavelengths in the Fano resonance (see Fig. 2d). Dimensions of the different elements are as in the asymmetric configuration depicted in Fig. 2.
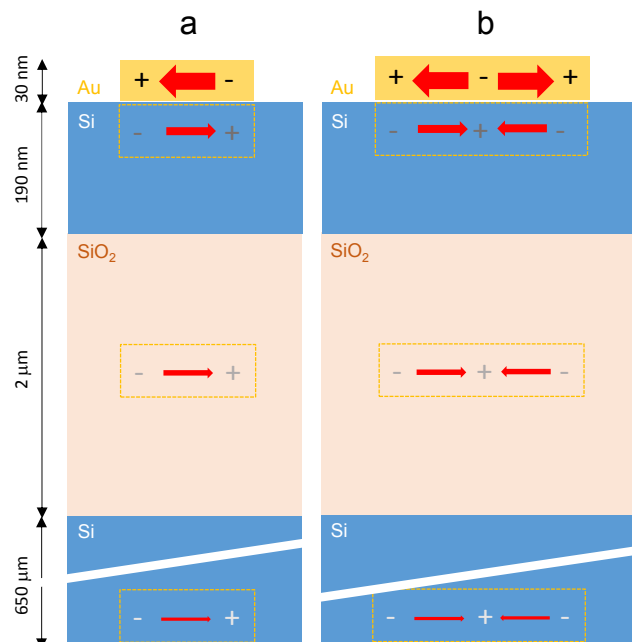

Figure 5. Schematic representation of the image currents in a system consisting of a plasmonic nanostrip (supporting a dipolar (a) or a quadrupolar (b) electric resonance) on top of a silicon-on-insulator wafer (dimensions not to scale). Accumulation of charges is represented by '+' or '-' signs whilst the arrows stand for the currents (and the thickness of the arrows stand for the current strength).
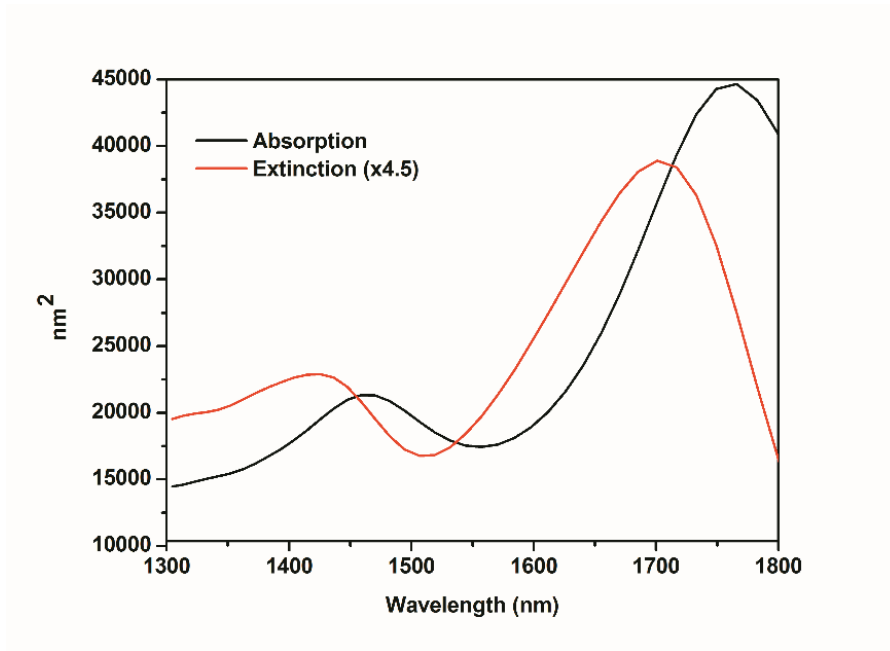
Figure 6. Nanostrip's scattering spectra illuminated with a plane wave and surrounded by an effective refractive index $n_{eff}=2.32$. The dimensions of the coupled systems are as in the asymmetric configuration of Fig. 2.

4. Discussion

Our previous results show the possibility to build plasmonic Fano nanoresonators showing narrower and steeper spectral features than the plasmonic electric dipole. However, as mentioned above, sharp and narrow spectral response is mandatory but not sufficient for practical applications. In addition, we need for deep transmission dips that result in large extinction ratios at the output. As mentioned above, adding more resonators is the most straightforward way to increase the extinction ratio regardless of the response of an isolate nanostructure (see Fig. 1c for the case of the short nanostrip response). We have performed similar calculations for the case of coupled-systems showing Fano response. To this end, a chain of five resonators – comprising each one a coupled Fano system - separated 155nm was computed. With this configuration the extinction ratio η increased from around 0.04, when only one resonator is considered, up to 0.17, as presented in Fig. 7. Since increasing the number of resonators along the waveguide increases the depth of the transmission dip, it would be helpful to calculate how many resonators would be needed to achieve transmission small enough for application purposes. In general, if we neglect interaction between adjacent resonators, the total transmission across a chain of m resonators can be obtained as $(1-\eta_0)^m$, η_0 being the extinction of a single element. In the case of the dipolar LSPR shown in Fig. 1, $\eta_0 = 0.12$ per resonator, we obtain that ~18 (~36) elements – with total lengths of ~30 μm (~60 μm) - would

be needed to get an extinction ration of 10 (20) dB, which would be large enough for applications such as switching. Since in the case of the Fano resonances and EIT behavior is η_0 reduced, even more resonators would be needed to get such large values of the extinction ratio. However, and taking into account application in sensing or switching, the sharpest spectral response of the Fano resonance should contribute to increase the sensitivity of the sensors or to reduce the required energy for switching. Notice also that larger values of the extinction ratio for a single nanostructure can be achieved by increasing the interaction strength, which can be done for instance by embedding the resonator inside a waveguide gap [19]. We envisage that combining the gap approach presented in [19] with the Fano/EIT approach discussed in this work could lead to deeper and sharper LSPRs, which could be a successful route for on-chip efficient processing elements with subwavelength footprint for sensing and switching purposes.
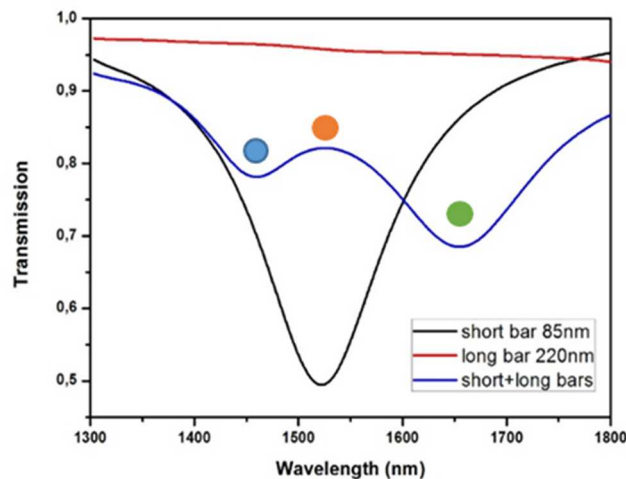

Figure 7. Transmission for the asymmetric configuration showing Fano and EIT behavior for a chain of five resonators separated 155nm. The extinction ratio is greatly enhance whilst the Fano asymmetric profile is maintained.

5. Conclusions

In conclusion, we have shown the onset of Fano resonances by the coupling between the bright and dark modes supported by a pair of gold nanostrips placed on top of a dielectric waveguide, giving rise, moreover, to the EIT phenomenon under certain conditions. By carefully choosing the length and position of the long nanostrip, the Fano resonance regime can be controlled. Although here demonstrated for telecom wavelengths, the same approach could be used in the visible regime by using silicon nitride waveguides and downscaling the metallic elements [15][16]. Finally, we would like to notice that recent approaches have shown how to get Fano resonances in plasmonic nanostructures coupled to plasmonic waveguides [33]-[36]. Our hybrid

plasmonic-photonic approach (in the sense that we consider a dielectric waveguide coupled to a metallic system [9]) has some remarkable advantages over such all-plasmonic approaches, mainly the use of low-loss dielectric waveguides that would enable to interconnect many different resonators spaced mm-scale distances on a single chip as well as the possibility of fabrication using well established semiconductor tools and processes.

Acknowledgements

References

[1] Maier S A 2007 *Plasmonics: Fundamentals and Applications* (New York: Springer)

[2] Schuller J A, Barnard E S, Cai W, Jun Y C, White J S and Brongersma M L 2010 Plasmonics for extreme light concentration and manipulation *Nature Mater.* 9 193-204.

[3] Zijlstra P, Paulo P M R and Orrit M 2012 Optical detection of single non-absorbing molecules using the surface plasmon resonance of a gold nanorod *Nature Nanotechnol.* 7 379-382.

[4] Kauranen M and Zayats A V 2012 Nonlinear plasmonics *Nature Photon.* 6 737-748.

[5] Husnik M Niegemann J Busch K and Wegener M 2013 Quantitative spectroscopy on individual wire, slot, bow-tie, rectangular, and square-shaped optical antennas *Opt. Lett.* 38 4597-4600.

[6] Fan P, Yu S, Fan S and Brongersma M L 2014 Optical Fano resonance of an individual semiconductor nanostructure *Nature Mater.* 13, 471–475.

[7] Rodríguez-Fortuño F J, Martínez-Marco M, Tomás-Navarro B, Ortuño R, Martí J, Martínez A and Rodríguez-Cantó P J 2011 Highly-sensitive chemical detection in the infrared regime using plasmonic gold nanocrosses *Appl. Phys. Lett.* 98 133118.

[8] Lorente-Crespo M, Wang L, Ortuño R, Garcia Meca C, Ekinci Y and Martínez A 2013 Magnetic Hot Spots in Closely Spaced Thick Gold Nanorings *Nano Lett.* 13 2654–2661.

[9] Rodríguez-Fortuño F J, Espinosa-Soria A and Martínez A 2016 Exploiting metamaterials, plasmonics and nanoantennas concepts in silicon photonics *J Opt.* 18, 123001.

[10] Lipson M 2005 Guiding, modulating, and emitting light on silicon - Challenges and opportunities *J. Lightwave Technol.* 23 4222–4238.

[11] Editorial Focus on "Silicon Photonics" 2010 *Nature Photon.* 4 491.

[12] Alepuz-Benache I, García-Meca C, Rodríguez-Fortuño F J, Ortuño R, Lorente-Crespo M, Griol A and Martínez A 2012 Strong magnetic resonance of coupled aluminum nanodisks on top of a silicon waveguide *Proc. SPIE* 8424 84242J.

[13] Arango F B, Kwadrin A and Koenderink A F 2012 Plasmonic antennas hybridized with dielectric waveguides *ACS Nano* 6, 10156–10167.

[14] Février M, Gogol P, Aassime A, Mégy R, Delacour C, Chelnokov A, Apuzzo A, Blaize S, Lourtioz J-M and Dagens B 2012 Giant coupling effect between metal nanoparticle chain and optical waveguide. *Nano Lett.* 12 1032–7.

[15] Chamanzar M, Xia Z, Yegnanarayanan S and Adibi A 2013 Hybrid integrated plasmonic-photonic waveguides for on-chip localized surface plasmon resonance (LSPR) sensing and spectroscopy *Opt. Express* 21 32086

[16] Peyskens F, Subramanian A Z, Neutens P, Dhakal A, Van Dorpe P, Le Thomas N and Baets R 2015 Bright and dark plasmon resonances of nanoplasmonic antennas evanescently coupled with a silicon nitride waveguide *Opt. Express* **23** 30885

[17] Peyskens F, Neutens P, Dhakal A, Van Dorpe P, Le Thomas N and Baets R 2016 Surface enhanced Raman spectroscopy using a single mode nanophotonic-plasmonic platform *ACS Photon.* 3, 102–108.

[18] Castro-Lopez M, de Sousa N, Garcia-Martin A, Gardes F Y and Sapienza R 2015 Scattering of a plasmonic nanoantenna embedded in a silicon waveguide *Opt. Express* 23 28108.

[19] Espinosa-Soria A, Griol A and Martínez A 2016 Experimental measurement of plasmonic nanostructures embedded in silicon waveguide gaps *Opt. Express* 24 9592

[20] Verellen N, Sonnefraud Y, Sobhani H, Hao F, Moshchalkov V V, Dorpe P V, Nordlander P and Maier S A 2009 *Nano Lett.* 9 1663.

[21] Luk'yanchuk B, Zheludev N I, Maier S A, Halas N J, Nordlander P, Giessen H and Chong C T 2010 The Fano resonance in plasmonic nanostructures and metamaterials *Nature Mater.* 9 707–15.

[22] Shafiei F, Monticone F, Le K Q, Liu X-X, Hartsfield T, Alù A and Li X 2013 A subwavelength plasmonic metamolecule exhibiting magnetic-based optical Fano resonance *Nature Nanotechnol.* 8, 95–99.

[23] Yang Z-J, Zhang Z-S, Zhang L-H, Li Q-Q, Hao Z H and Wang Q-Q 2011 Fano resonances in dipole-quadrupole plasmon coupling nanorod dimers *Opt. Lett.* 36, 1542-1544.

[24] Liu N, Langguth L, Weiss T, Kästel J, Fleischhauer M, Pfau T and Giessen H 2009 Plasmonic analogue of electromagnetically induced transparency at the Drude damping limit *Nature Mater.* 8, 758–762.

[25] Harris S E 1997 Electromagnetically induced transparency *Phys. Today* 50, 36–42.

[26] Wu C, Khanikaev A B, Adato R, Arju N, Yanik A A, Altug H, Shvets G 2012 Fano-resonant asymmetric metamaterials for ultrasensitive spectroscopy and identification of molecular monolayers *Nature Mater*. 11, 69–75.

[27] Chang W S, Lassiter J B, Swanglap P, Sobhani H, Khatua S, Nordlander P and Halas NJ, 2012 A Plasmonic Fano Switch *Nano Lett.* 12, 4977–4982.

[28] Espinosa-Soria A and Martínez A 2016 Transverse Spin and Spin-Orbit Coupling in Silicon Waveguides *IEEE Photon. Technol. Lett.* 28, 1561-1564.

[29] Amin M, Farhat M and Bağcı H 2013 A dynamically reconfigurable Fano metamaterial through graphene tuning for switching and sensing applications *Sci. Rep.* 3, 2105.

[30] Knight M W, Wu Y, Lassiter J B, Nordlander P and Halas N J 2009 Substrates matter: influence of an adjacent dielectric on an individual plasmonic nanoparticle *Nano Lett.* 9 2188–92

[31] Valamanesh M, Borensztein Y, Langlois C and Lacaze E 2011 Substrate effect on the plasmon resonance of supported flat silver nanoparticles *J. Phys. Chem. C* 115 2914–22

[32] Berkovitch N, Ginzburg P and Orensteinet M 2012 Nano-plasmonic antennas in the near infrared regime *J. Phys.: Condens. Matter* 24 073202

[33] Lu H, Liu X, Mao D and Wang G 2012 Plasmonic nanosensor based on Fano resonance in waveguide-coupled resonators *Opt. Lett.* 37, 3780-3782.

[34] Chen J, Sun C and Gong Q 2014 Fano resonances in a single defect nanocavity coupled with a plasmonic waveguide *Opt. Lett.* 39, 52-55.

[35] Yun Binfeng, Guohua Hu, Ruohu Zhang and Cui Yiping 2016 *J. Opt.* 18 055002.

[36] Bing-Hua Zhang, Ling-Ling Wang, Hong-Ju Li, Xiang Zhai and Sheng-Xuan Xia 2016 *J. Opt.* 18 065001.